Speciation of Uranium in Sediments before and after In situ Biostimulation

SHELLY D. KELLY,*,† KENNETH M. KEMNER,† JACK CARLEY,‡ CRAIG CRIDDLE,§ PHILLIP M. JARDINE,‡ TERENCE L. MARSH,⊥ DEBRA PHILLIPS,|| DAVID WATSON,‡ AND WEI-MIN WU§

Biosciences Division, Argonne National Laboratory, 9700 South Cass Avenue, Argonne, Illinois 60439-4843, Environmental Sciences Division, Oak Ridge National Laboratory, P. O. Box 2008, Oak Ridge, Tennessee 37831, Department of Civil and Environmental Engineering, Stanford University, Stanford, California 94305-4020, Microbiology and Molecular Genetics, Michigan State University, 2215 Biomedical Physical Sciences, East Lansing, Michigan 48824-4320, Environmental Engineering Research Centre, School of Planning, Architecture, and Civil Engineering, Queen's University of Belfast, Belfast BT9 5AG, Northern Ireland, United Kingdom

Received July 17, 2007. Revised manuscript received October 3, 2007. Accepted December 10, 2007.

The success of sequestration-based remediation strategies will depend on detailed information, including the predominant U species present as sources before biostimulation and the products produced during and after in situ biostimulation. We used X-ray absorption spectroscopy to determine the valence state and chemical speciation of U in sediment samples collected at a variety of depths through the contaminant plume at the Field Research Center at Oak Ridge, TN, before and after approximately 400 days of in situ biostimulation, as well as in duplicate bioreduced sediments after 363 days of resting conditions. The results indicate that U(VI) in subsurface sediments was partially reduced to 10–40% U(IV) during biostimulation. After biostimulation, U was no longer bound to carbon ligands and was adsorbed to Fe/Mn minerals. Reduction of U(VI) to U(IV) continued in sediment samples stored under anaerobic condition at <4 °C for 12 months, with the fraction of U(IV) in sediments more than doubling and U concentrations in the aqueous phase decreasing from 0.5−0.74 to <0.1 μM. A shift of uranyl species from uranyl bound to phosphorus ligands to uranyl bound to carbon ligands and the formation of nanoparticulate uraninite occurred in the sediment samples during storage.

Introduction

Nuclear weapons production resulted in the storage of vast quantities of nuclear waste at former U.S. weapons complex sites. Many of these storage areas have generated large subsurface contaminant plumes of U, Tc, and/or Cr, along with extreme ionic strength and pH values. Current remediation strategies for large subsurface plumes of U and other heavy metals focus on sequestration of the contaminants within the subsurface by reducing U(VI) to U(IV). Isolated cultures in laboratory studies have identified indigenous dissimilatory metal-reducing bacteria that can rapidly remove aqueous U(VI) through the formation of poorly crystalline U(IV) oxide precipitates (*1, 2*) and sulfate-reducing bacteria (SRB) that are capable of removing U(VI) from solution (*3–8*). In two of these studies, uraninite as a product of sulfate-reducting conditions was identified through TEM images (*5, 6*). Field experiments to test in situ bioreduction of U identified a decrease of aqueous U(VI) but did not characterize the sediment-phase U species (*3, 9–11*), whereas another study verified the presence of some solid-phase U(IV) (*12*). Enrichment of field site materials in laboratory studies has also verified a decrease in U(VI) aqueous concentrations (*13, 14*), and in several instances solid-phase U(IV) has been confirmed (*15–19*), but few studies have characterized the U(IV) species. In some systems, U(VI) has been shown to persist in the solid phases during microbial reduction (*5, 15, 19, 20*).

Hexavalent U can also be reduced to tetravalent U through abiotic processes that may or may not be associated with microbial activities. In the presence of low carbonate concentration, sulfide, which is the end product of sulfate reduction by SRB, reduces U(VI) hydroxyl species to U(IV) as uraninite particles (*21*). Mixed Fe(II)−Fe(III) oxyhydroxides in the form of green rusts found in suboxic environments have also been shown to reduce U(VI) via the formation of U(IV) oxide nanoparticles (*22*). Fe(II) associated with surrogate cell wall components has also been shown to reduce U(VI) (*23*).

The success of sequestration-based remediation strategies will depend on detailed information, including the major U sources within the sediments throughout a contaminated volume containing a heterogeneous mixture of sediment and aqueous phases. X-ray absorption fine structure (XAFS) spectroscopy is ideally suited for these types of investigations, as measurements can be made on unaltered sediments under anoxic conditions.

A pilot-scale in situ study of U bioremediation/immobilization has been conducted since August 2003 at the high U-contaminated Field Research Center at Oak Ridge, TN (*12, 24*). U(VI) was partially reduced through biostimulation of microbial activity by the addition of ethanol as electron donor to the subsurface (*12*). In this study, we used XAFS spectroscopy to determine the valence state and chemical speciation of U in the sediment samples collected before biostimulation and after approximately 400 days of biostimulation. The results provide unique information on the shift of chemical speciation of U throughout the plume during biostimulation. We also demonstrate continued U(VI) reduction and U species transformations in sediment samples stored under anoxic conditions at temperature <4 °C.

Materials and Methods

Site Description. The Field Research Center (FRC) field site is adjacent to the former S-3 Ponds at the Y-12 National Security Complex, Oak Ridge, TN. These ponds were 121 m by 121 m by 5 m deep and received 10 ML of waste per year in 1951–1983, including NO_3^-, U, ^{99}Tc, and other metals at pH < 2.0 (*25*). Though subsequently covered with an asphalt parking lot, the ponds have created a U plume with sediment U concentrations up to 800 mg kg^{-1} (*26*). The in situ

* Corresponding author phone: (630) 252-7376; fax: (630) 252-9793; e-mail: skelly@anl.gov.
† Argonne National Laboratory.
‡ Oak Ridge National Laboratory.
§ Stanford University.
⊥ Michigan State University.
|| Queen's University of Belfast.

10.1021/es071764i CCC: $37.00
Published on Web 01/25/2008

TABLE 1. Samples from the Y-12 National Security Complex, Oak Ridge, TN, Used in This Study[a]

name	location	sample	date collected from field	date of EXAFS data collection	depth (m)	color when EXAFS data collected
Core Sediments Collected before Biostimulation						
MLS0–14A-B	FW100	FWB100–06–12A	Nov 2001	9 March 2003	14.0	blackish
MLS0–14G-B		FWB100–06–12G (replicate)	Nov 2001		14.0	blackish
MLS0–13.7-B		FWB100–06–03	Nov 2001		13.7	greenish gray
MLS1–12.2-B	FW101	FWB101–08–12	Nov 2001		12.2	brownish
Surged Sediments within Serum Bottle Containing Groundwater and Solid Phases Collected during Biostimulation Each with Duplicate Serum Bottle						
MLS1–13.7-D	FW101	FW101–2	3 March 2005 (day 559)	23 March 2005	13.7	tan
MLS1–12.2-D		FW101–3	3 March 2005 (day 559)		12.2	tan
INJECT-12.2-D	FW104	FW104	8 Feb 2005 (day 535)		12.2	black
Duplicate Serum Bottles of Surged Sediments Stored <4 °C for Approximately 1 Year						
MLS1–13.7-A	FW101	FW101–2	3 March 2005 (day 559)	20 March 2006	13.7	dark green
MLS1–12.2-A		FW101–3	3 March 2005 (day 559)		12.2	dark green
INJECT-12.2-A	FW104	FW104	8 Feb 2005 (day 535)		12.2	black

[a] Pilot-scale in situ bioremediation/immobilization of U began on 24 Aug 2003 (day 1) with preconditioning. Biostimulation through ethanol injection began on 7 Jan 2004 (day 137).

biostimulation wells include the injection well FW104 for ethanol delivery and multilevel sampling wells (MLSs) FW100, and FW101 to monitor the performance of the bioremediation. A brief summary of the in situ biostimulation project is given in the Supporting Information, Section S1.

Sample Collection and Preparation. Sediment samples are summarized in Table 1. Prior to field tests (November 2001), four core sediment samples were taken under suboxic conditions as described elsewhere (*27*) during drilling of FW100 and FW101. The sediment sample (FWB101–08–12) from FW101 at 12.2 m had a brownish color. The core sample (FWB100–06–03) was collected from near the bottom of FW100 at 13.7 m and had a greenish-gray color. Samples from FW100 at 14.0 m are FWB100–06–12A and replicate FWB100–06–12G (both blackish). We selected these samples for study because they contained high levels of U (730 mg/kg in FWB100–06–12A/G, 164 mg/kg in FWB100–06–03, and 156 mg/kg in FRB101–08–12) and were located in the target region to be tested for bioremediation (*24*). A brief description of the sediment mineralogy is given in the Supporting Information, Section S2.

Because of the technical difficulty of taking core samples at locations where previous cores have been taken, sediment samples were retrieved during biostimulation from inner-loop injection well FW104 and MLS well FW101 by using a surge block to extract sediment samples from the matrix surrounding the well screen at the locations of the core samples (*24*). The sample from FW104 was taken on February 8, 2005 (operational day 535), at 12.2 m (FW104). The other two samples were collected from MLS well FW101 on March 3, 2005 (operational day 559), at 12.2 (FW101–3) and 13.7 m (FW101–2). We did not take samples from FW100, because there was no microbial reduction activity in that MLS at that time, as evidenced by the aqueous chemistry within the wells. In this manuscript, the sediment samples are given names beginning with "MLS0," "MLS1," or "INJECT" to indicate FW100, FW101, or FW104, respectively. The initial string is followed by "−14," "−13.7," or "−12.2" to denote the depth in meters from which the sample was collected, then by "-B" to denote core samples collected before bioremediation, "-D" to denote surged samples collected during bioremediation, or "-A" to denote duplicates of the surged samples collected during bioremediation after storage for approximately one year. The replicate samples at 14.0 m are distinguished by an additional "A" or "G" for samples FWB100–06–12A or FWB100–06–12G, respectively. These sample names are summarized in Table 1.

Measurement Methods. The Supporting Information contains the description of the analytical methods for determining groundwater anions and cations, Fe(II), and U concentrations (the Supporting Information, Section 3), a description of the surged samples containing groundwater and sediments stored under inert atmosphere (Supporting Information, Section 4), the MRCAT beamline parameters used for the X-ray beamline setup and XAFS data collection (Supporting Information, Section 5), the XANES analysis methods by linear combination fitting and by the number of axial oxygen atoms of the uranyl (Supporting Information, Section 6), the general EXAFS methods (Supporting Information, Section 7), and the details of the EXAFS models including the paths and constraints (Supporting Information, Section 8).

Results and Discussion

Groundwater Geochemistry. The geochemical properties of groundwater in injection well FW104 and monitoring well FW101 before biostimulation, during biostimulation, and after a year of storage are summarized in Table S1 of the Supporting Information. Details of changes in aqueous chemistry during biostimulation are given elsewhere (*12, 24*). Briefly, nitrate concentrations decreased from 113−208 to ~0.04 mM (Table S1 of the Supporting Information) by in situ denitrification (*24*). During preconditioning, U concentration was reduced from approximately 150 to 3 μM by clean-water flushing, then reduced to 0.74 μM or less during ethanol injection to stimulate microbial activity (Table S1 of the Supporting Information). The sulfide concentration increased from below detection limits to 0.01–0.1 mM in MLS during ethanol injection.

The surged sediment sample INJECT-12.2-D was black, and samples from MLS1–12.2-D and MLS1–13.7-D were tan colored. The process of surging the wells during biostimulation resulted in varying colors within the extracted sediments depending on the duration between surging procedures and the amendments. Samples surged on day 535 from FW101–2 were greenish (*12*), whereas the samples for this study surged on day 559 were tan colored. The U concentration within the sediment samples MLS1–13.7-D, MLS1–12.2-D, and INJECT-12.2-D were 0.96, 1.02, and 2.28 g/kg of dry solids, respectively. The higher U content in INJECT-12.2-D samples than in MLS1-D samples reflects greater accumulation of U near the injection well.

One of the three serum bottles (INJECT-12.2-D/A) showed an increase in total aqueous Fe concentration from 0.01 mM during biostimulation to 0.10 mM after a year of storage with 0.04 mM aqueous Fe(II) after storage (Table S1 of the Supporting Information). The aqueous phases within the other two MLS1 serum bottles showed a decrease or little

change in the total Fe concentration from during biostimulation compared to after a year of storage. Aqueous phase sulfate concentrations within all serum bottles decreased from 0.2−0.4 mM to 0.004–0.02 mM after a year of storage (Table S1 of the Supporting Information).

During storage at <4 °C, the aqueous U concentration dropped from 0.5−0.7 μM during biostimulation to 0.02–0.1 μM (Table S1 of the Supporting Information), well below the maximum contaminant level (MCL) for drinking water promulgated by the U.S. Environmental Protection Agency (U.S. EPA), indicating that, within this closed system, aqueous U reduction/immobilization can occur even at low temperatures under anoxic conditions. On the basis of the decrease in aqueous [U] during storage, the solid-phase [U] is expected to increase by only 0.03 mg/kg dry solids.

Average U Valence State within Sediments. Before biostimulation, the U L_{III}-edge XANES spectra from the MLS1–12.2-B, MLS0–13.7-B, and MLS0–14A/G-B sediment samples collected in March 2002 indicate 100 ± 10% U(VI) (Figure S3 of the Supporting Information). This indicates no reduced U in the target treatment area before biostimulation, although sample MLS0–13.7-B and replicate samples MLS0–14A/G-B had greenish-gray and blackish colors, respectively.

Sediment samples collected after approximately 400 days of biostimulation indicate approximately 92 ± 10, 85 ± 10, and 57 ± 10% U(VI), with the remainder as U(IV), in sediments samples MLS1–13.7-D, MLS1–12.2-D, and INJECT-12.2-D, respectively (Table S2 of the Supporting Information). This result confirms that reduction of U(VI) occurred not only near injection well FW104, but also around monitoring well FW101. No unique U(IV) phase could be detected in the FW101 spectra, probably because of the poor data quality and the small percentage of the U(IV) phase (8–23% ± 10%). Previous XANES studies (*12*) of a sediment sample taken from FW101–2 on day 535 found more reduced U [65% U(IV)] in the greenish sediments, whereas our tan colored sediments taken on day 559 contained only 8% U(IV). The large differences between the surged samples could be caused by variability in the rate and extent of surging in the well. The abundant reduced U(IV) surged on day 535 could have accumulated on the surface of sediment matrix until it was removed by the surging operation on that day.

The U L_3-edge XANES spectra for sediments collected after biostimulation and stored for approximately one year at <4 °C indicate approximately 66 ± 10%, 68 ± 10%, and 35 ± 10% U(VI), with the remainder as U(IV), in the sediment samples MLS1–13.7-A, MLS1–12.2-A, and INJECT-12.2-A, respectively (Table S2 of the Supporting Information). These results confirm that reduction of U(VI) continued in the refrigerator under anoxic conditions. The fractions of Oax atoms, measured independently on the basis of EXAFS spectra are consistent with the results from linear-combination fitting of the XANES spectrum (Table S2 of the Supporting Information).

Uranyl Species. Figures 1−3 summarizes the U L_3-edge EXAFS spectra and the predominant U species for the samples collected before and during biostimulation, as well as the duplicate samples collected during biostimulation and stored under anoxic conditions for approximately one year. These Figures show the EXAFS fitting results for the coordination numbers and distances for each ligand type. The analysis of the EXAFS spectra for samples collected before biostimulation (MLS1–12.2-B and MLS0–14A-B) (panels A and C in Figure 1) indicates that uranyl is predominantly bound to monodentate phosphorus and bidentate carbon ligands. The EXAFS results are consistent with uranyl bound to the surface of a mineral (*28, 29*) or a ligand from organic matter (*30–32*), rather than the formation of uranyl precipitates. In contrast, the EXAFS spectra analysis for sediment sample MLS0–13.7-B (Figure 1B) shows a small amount of a uranyl-oxide-like structure (18 ± 13%), in addition to some C-containing ligands. No P-containing ligands bound to uranyl were needed to model the EXAFS spectra from the MLS0–13.7-B sediment.

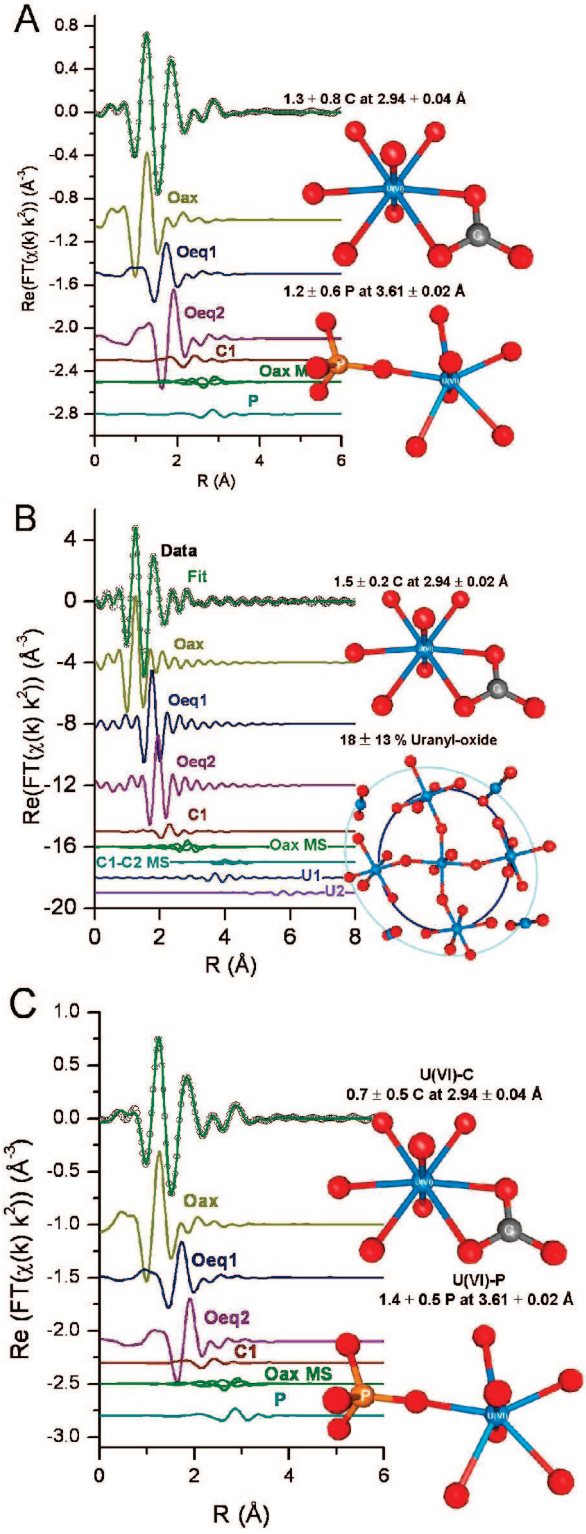

FIGURE 1. Real part of the Fourier transform of the U L_{III}-edge EXAFS spectrum (open symbols) and the EXAFS model (green line), with the components of the model offset under the EXAFS spectrum. The major U species are depicted next to each spectrum. The data shown are for sediment samples before biostimulation: (A) MLS1–12.2-B, (B) MLS0–13.7-B, and (C) MLS0–14A-B.

A previous study identified uranium phosphates as discrete precipitates having characteristics similar to those

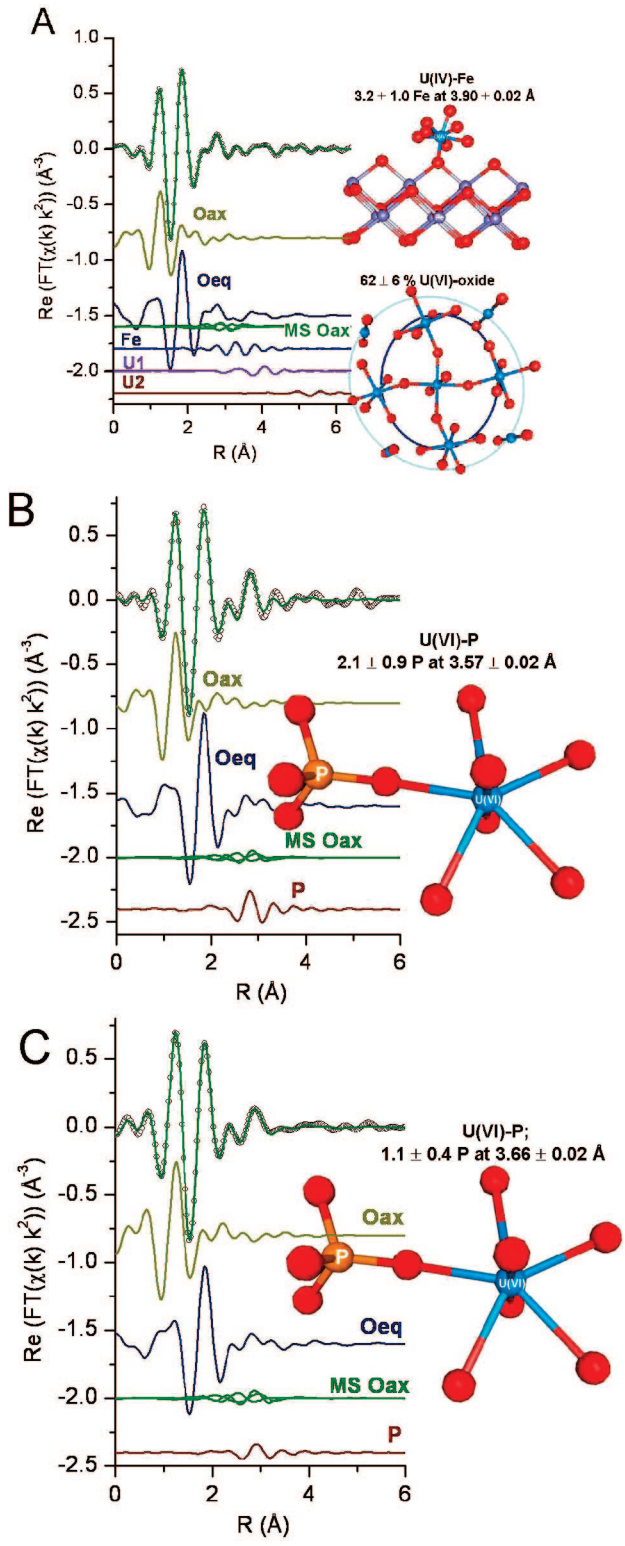

FIGURE 2. Real part of the Fourier transform of the U L_{III}-edge EXAFS spectrum (open symbols) and the EXAFS model (green line), with the components of the model offset under the EXAFS spectrum. The major U species are depicted next to each spectrum. The data shown are for samples during biostimulation: (A) INJECT-12.2-D, (B) MLS1–12.2-D, and (C) MLS1–13.7-D.

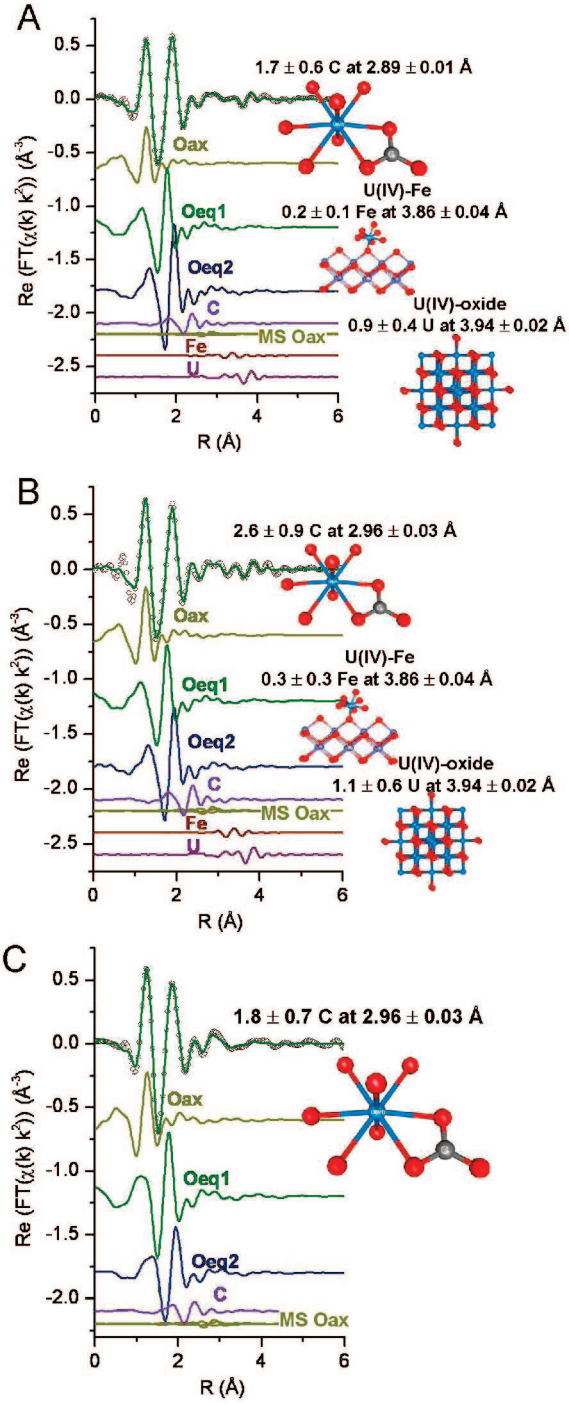

FIGURE 3. Real part of the Fourier transform of the U L_{III}-edge EXAFS spectrum (open symbols) and the EXAFS model (green line), with the components of the model offset under the EXAFS spectrum. The major U species are depicted next to each spectrum. The data shown are for the same samples as in Figure 2 after storage at <4 °C: (A) INJECT-12.2-A, (B) MLS1–13.7-A, and (C) MLS1–12.2-A.

of the autunite and meta-autunite groups in samples from FWB103 at the 12.2 and 12.8 m depths (*33*). However, XRD of samples from those depths failed to identify uranium phosphates, perhaps because concentrations of the U-P minerals were below detection limits (*26*). Uranium phosphate complexes on mineral grains are likely, because uranium and phosphate are products of previous waste disposal at the S-3 ponds site (*25*). Uranium carbonates were also identified in samples from this study. The carbonates are from the calcium carbonate-rich bedrock at the site, particularly at depths below about 14 m (*26*).

No C-containing ligands were detected in the EXAFS spectra for sediment samples collected during biostimulation from wells FW104 and FW101 (Figure 2). Sediments

MLS1–13.7-D and MLS1–12.2-D indicate the dominance of uranium bound to P-containing ligands (panels B and C in Figure 2). In contrast, the sample taken from INJECT-12.2-D showed ~60% of the U as a uranyl-oxide-like phase and ~40% as U(IV) associated with Fe/Mn atoms (Figure 2A). After the sediments collected during biostimulation were stored in serum bottles at 4 °C for 12−13 months, the uranyl carbonate species was again detected as the dominant uranium species (Figure 3). All three stored samples showed an increase in the total percentage of U(IV) (Table S2 of the Supporting Information), and two samples showed significant uraninite species (Figure 3). The mechanism responsible for these changes in U speciation is unclear, but it is likely related to continuous U(VI) reduction under anaerobic conditions in the closed system where the fine sediment particles are in contact with groundwater. On the basis of the postbiostimulation results, an attempt was made to use the U−Fe signal to model these spectra. The amplitude of this signal was above background only for sample INJECT-12.2-A. Detailed discussions of our EXAFS results are given in the Supporting Information, Section 9.

Biostimulation and Uranium Phosphate Species. Two of the three prebiostimulation sediment samples can be modeled with a significant U-P signal (Figure 1). Two of the three sediment samples collected during biostimulation again showed a U-P signal (Figure 2). These results suggest that the uranyl phosphate phase was resistant to bioreduction during the subsurface treatment applied in this study (*12*). Interestingly, after the sediments were stored at 4 °C for one year, U−P signals were not detected in measured spectra (Figure 3), indicating that under conditions present during storage the U−P species can be transformed.

Biostimulation and Uranium Carbonate Species. Sediment samples collected before biostimulation were characterized by a strong U-C EXAFS signal. The number of C atoms bound to the uranyl species before biostimulation ranged from 0.5 to 1.7 (Figure 1). The existence of a uranyl carbonate species is supported by its removal during biostimulation, because no U-C signal was detected in the sediments collected during biostimulation (Figure 2). Because of its greater solubility, uranyl carbonate species might have been more easily reduced than uranyl phosphorus species. After a year in storage, all three bioreduced samples showed a significant U−C signal but no U-P signal (Figure 3). The source of the carbon forming the complex with U could be aqueous bicarbonate (~3 mM) that has adsorbed to solid phase (*34*) or carboxyl groups associated with biomass (*30–32*). In contrast to the sediment matrix in the subsurface, the sediment samples stored in serum bottles were in slurry form with good contact between solid and aqueous phases.

Reduced Uranium Species. The U(IV) mineral uraninite was expected to be present in the sediment samples collected during biostimulation. Previous laboratory studies showed the EXAFS technique to be capable of identifying nanoparticulate uraninite as the product of biostimulation (*18*), as well as a product of reduction by mixed Fe(II)/Fe(III) oxyhydroxides (*22*). However, in the present study, EXAFS models based on the uraninite structure failed to reproduce the measured spectra from the sediments collected during biostimulation. Instead of uraninite, the EXAFS spectra support U(IV) in association with Fe/Mn (Figure 2). The adsorption of U(IV) to Fe and/or Mn oxide coatings is supported by the previous identification of these coatings within these sediments (*26*). Both biotic and abiotic reduction of U(VI) to U(IV) has been shown to produce uraninite nanoparticles in simplified laboratory systems (*18, 22*), whereas more complex systems have yielded other U(IV) species (*23*) or incomplete U(VI) reduction (*20*). In a simplified laboratory study, U(VI) reduction by Fe(II) yielded a U(IV)−Fe complex (*23*) with the U(IV)−Fe distance of the common bidentate coordination, unlike our proposed monodentate coordination (see the Supporting Information, Section 9.5). These studies illustrate the complexity of the redox chemistry of U in natural systems.

Impact of Storage. After a year of storage, the percentage of U(IV) in the solid phase increased from 38−43 to 63–65% for sample INJECT-12.2-D to INJECT-12.2-A, 8–11 to 44–50% for sample MLS1–13.7-D to MLS1–13.7-A, and 15–23 to 42–50% for sample MLS1–12.2-D to MLS1–12.2-A (Table S2 of the Supporting Information) and two of the three samples showed evidence of uraninite after storage (Figure 3). The groundwater chemistry is similar before and after a year of storage (Table S1 of the Supporting Information). The most notable change is a decrease in the concentration of aqueous sulfate and uranium. We do not have additional information to directly connect the biogeochemical processes causing the decrease in aqueous sulfate and the decrease in aqueous uranium. These results demonstrate that reduction of U(VI) to U(IV) can continue even at temperature <4 °C.

Implications for Bioremediation. The continuation of abiotic/biotic processes within the stored sediments and their effect of decreasing aqueous U concentrations to levels less than the U.S. EPA MCL may be a promising result for in situ bioremediation strategies. The connection between results for (*1*) our closed porous system containing fine particulate sediments in contact with groundwater and (*2*) the open in situ system in the field containing weathered saprolite dominated by preferential groundwater flow paths is uncertain. However, our observed U transformations may be facilitated by mass transfer within the closed system that could be overcome by additional time in the open system. Indeed, recently collected sediments from the open in situ system have confirmed many of the U transformations found in our closed system (data not shown), indicating that mass transfer effects could be partially responsible for the longer time needed to affect the in situ system.

An understanding of the biogeochemical processes that give rise to changes in the speciation of U as a result of natural attenuation or biostimulation approaches is necessary for making informed decisions concerning remediation and long-term stewardship strategies at contaminated sites. Results from these biostimulation experiments (*13*) demonstrate that in situ biostimulation of subsurface material can facilitate the removal of U from groundwater to the solid phase via reductive precipitation and/or sorption processes. The results also demonstrate that homogenization of subsurface material may facilitate more extensive reduction and a shift in the partitioning of the speciation of U, possibly because of enhanced interaction between groundwater and solid-phase surfaces due to increased surface area. These results provide some insight into the importance of heterogeneities and mass transfer rates through the subsurface and their role in controlling the chemical speciation of contaminant metals and radionuclides. Specifically, these results suggest that extended amounts of time (i.e., years) may be needed before the vast majority of U-contaminated subsurface materials can be reduced in situ. Even though significant decreases in aqueous U occurred in situ within 400 days of biostimulation, the formation of uraninite was not detected in the samples collected from the field. Uraninite was detected in two of the three duplicate sediment samples after a year of storage. Thus, monitoring the speciation of U associated with solid-phase subsurface materials for extended periods of time (i.e., years) after biostimulation may be necessary. Clearly, additional studies are needed to improve understanding of these complicated in situ processes.

Acknowledgments

This work was supported by the U.S. Department of Energy (DOE), Office of Science, Office of Biological and Environmental Research, Environmental Remediation Sciences Program. MRCAT operations are supported by the U.S. DOE and the MRCAT member institutions. Advance Photon Source is supported by the U.S. DOE, Office of Science, Office of Basic Energy Sciences, under Contract DE-AC02-06CH11357. Special appreciation is extended to E. J. O'Loughlin (ANL) for helpful discussions and to M. Boyanov and B. Ravel (ANL) for assistance with the uranium XAFS data collection. The authors thank Dr. Baohua Gu, Hui Yan, and Kenneth Lowe for the analysis of groundwater samples.

Supporting Information Available

Details of the Biostimulation Project (Section S1), Sediment mineralogy (Section S2), Analytical Methods (Section S3), Description of Surged Sediments (Section S4), and XAS details in text (Section S5–S9), Tables S1−S13, and Figures S1−S10 (PDF). This material is available free of charge via the Internet at http://pubs.acs.org.

Literature Cited

(1) Lovley, D. R.; Phillips, E. J. P.; Gorby, Y. A.; Landa, E. R. Microbial reduction of uranium. *Nature* **1991**, *350* (6317), 413–416.

(2) Lovley, D. R.; Roden, E. E.; Phillips, E. J. P.; Woodward, J. C. Enzymatic iron and uranium reduction by sulfate-reducing bacteria. *Mar. Geol.* **1993**, *113* (1–2), 41–53.

(3) Holmes, D. E.; Finneran, K. T.; O'Neil, R. A.; Lovley, D. R. Enrichment of members of the family Geobacteraceae associated with stimulation of dissimilatory metal reduction in uranium-contaminated aquifer sediments. *Appl. Environ. Microb.* **2002**, *68* (5), 2300–2306.

(4) Min, M. Z.; Xu, H. F.; Barton, L. L.; Wang, J.; Peng, X. J.; Wiatrowski, H. Biomineralization of uranium: A simulated experiment and its significance. *Acta. Geol. Sin.* **2005**, *79* (1), 134–138.

(5) Suzuki, Y.; Kelly, S. D.; Kemner, K. M.; Banfield, J. F. Enzymatic U(VI) reduction by Desulfosporosinus species. *Radiochim. Acta* **2004**, *92* (1), 11–16.

(6) North, N. N.; Dollhopf, S. L.; Petrie, L.; Istok, J. D.; Balkwill, D. L.; Kostka, J. E. Change in bacterial community structure during in situ biostimulation of subsurface sediment cocontaminated with uranium and nitrate. *Appl. Environ. Microb.* **2004**, *70* (8), 4911–4920.

(7) Shelobolina, E. S.; Sullivan, S. A.; O'Neill, K. R.; Nevin, K. P.; Lovley, D. R. Isolation, characterization, and U(VI)-reducing potential of a facultatively anaerobic, acid-resistant bacterium from Low-pH, nitrate- and U(VI)-contaminated subsurface sediment and description of *Salmonella subterranea sp nov. Appl. Environ. Microbiol.* **2004**, *70* (5), 2959–2965.

(8) Petrie, L.; North, N. N.; Dolhoph, S. L.; Balkwill, D. L.; Kostka, J. E. Enumeration and characterization of iron(III)-reducing microbial communitities from acidic subsurface sediments contaminated with uranium(VI). *Appl. Environ. Microb.* **2003**, *69* (12), 7467–7679.

(9) Istok, J. D.; Senko, J. M.; Krumholz, L. R.; Watson, D.; Bogle, M. A.; Peacock, A.; Chang, Y. J.; White, D. C. In situ bioreduction of technetium and uranium in a nitrate-contaminated aquifer. *Environ. Sci. Technol.* **2004**, *38*, 468–475.

(10) Anderson, R. T.; Vrionis, H. A.; Ortiz-Bernad, I.; Resch, C. T.; Long, P. E.; Dayvault, R.; Karp, K.; Marutzky, S.; Metzler, D. R.; Peacock, A.; White, D. C.; Lowe, M.; Lovley, D. R. Stimulating the in situ activity of Geobacter species to remove uranium from the groundwater of a uranium-contaminated aquifer. *Appl. Environ. Microbiol.* **2003**, *69* (10), 5884–5891.

(11) Chang, Y. J.; Long, P. E.; Geyer, R.; Peacock, A. D.; Resch, C. T.; Sublette, K.; Pfiffner, S.; Smithgall, A.; Anderson, R. T.; Vrionis, H. A.; Stephen, J. R.; Dayvault, R.; Ortiz-Bernad, I.; Lovley, D. R.; White, D. C. Microbial incorporation of C-13-labeled acetate at the field scale: Detection of microbes responsible for reduction of U(VI). *Environ. Sci. Technol.* **2005**, *39* (23), 9039–9048.

(12) Wu, W. M.; Carley, J.; Gentry, T.; Ginder-Vogel, M. A.; Fienen, M.; Mehlhorn, T.; Yan, H.; Caroll, S.; Pace, M. N.; Nyman, J.; Luo, J.; Gentile, M. E.; Fields, M. W.; Hickey, R. F.; Gu, B. H.; Watson, D.; Cirpka, O. A.; Zhou, J. Z.; Fendorf, S.; Kitanidis, P. K.; Jardine, P. M.; Criddle, C. S. Pilot-scale in situ bioremediation of uranium in a highly contaminated aquifer. 2. Reduction of U(VI) and geochemical control of U(VI) bioavailability. *Environ. Sci. Technol.* **2006**, *40* (12), 3986–3995.

(13) Lee, B. D.; Walton, M. R.; Megio, J. L. Biological and chemical interactions with U(VI) during anaerobic enrichment in the presence of iron oxide coated quartz. *Water Res.* **2005**, *39* (18), 4363–4374.

(14) Abdelouas, A.; Lu, Y. M.; Lutze, W.; Nuttall, H. E. Reduction of U(VI) to U(IV) by indigenous bacteria in contaminated ground water. *J. Contam. Hydrol.* **1998**, *35* (1–3), 217–233.

(15) Nyman, J. L.; Marsh, T. L.; Ginder-Vogel, M. A.; Gentile, M.; Fendorf, S.; Criddle, C. Heterogeneous response to biostimulation for U(VI) reduction in replicated sediment microcosms. *Biodegradation* **2006**, *17* (4), 303–316.

(16) Suzuki, Y.; Kelly, S. D.; Kemner, K. M.; Banfield, J. F. Direct microbial reduction and subsequent preservation of uranium in natural near-surface sediment. *Appl. Environ. Microb.* **2005**, *71* (4), 1790–1797.

(17) Abdelouas, A.; Lutze, W.; Gong, W. L.; Nuttall, E. H.; Strietelmeier, B. A.; Travis, B. J. Biological reduction of uranium in groundwater and subsurface soil. *Sci. Total Environ.* **2000**, *250* (1–3), 21–35.

(18) Suzuki, Y.; Kelly, S. D.; Kemner, K. M.; Banfield, J. F. Radionuclide contamination - Nanometre-size products of uranium bioreduction. *Nature* **2002**, *419* (6903), 134–134.

(19) Gu, B. H.; Wu, W. M.; Ginder-Vogel, M. A.; Yan, H.; Fields, M. W.; Zhou, J.; Fendorf, S.; Criddle, C. S.; Jardine, P. M. Bioreduction of uranium in a contaminated soil column. *Environ. Sci. Technol.* **2005**, *39* (13), 4841–4847.

(20) Jeon, B. H.; Kelly, S. D.; Kemner, K. M.; Barnett, M. O.; Burgos, W. D.; Dempsey, B. A.; Roden, E. E. Microbial reduction of U(VI) at the solid-water interface. *Environ. Sci. Technol.* **2004**, *38* (21), 5649–5655.

(21) Hua, B.; Xu, H. F.; Terry, J.; Deng, B. L. Kinetics of uranium(VI) reduction by hydrogen sulfide in anoxic aqueous systems. *Environ. Sci. Technol.* **2006**, *40* (15), 4666–4671.

(22) O'Loughlin, E. J.; Kelly, S. D.; Cook, R. E.; Csencsits, R.; Kemner, K. M. Reduction of uranium(VI) by mixed iron(II)/iron(III) hydroxide (green rust): Formation of UO_2 nanoparticles. *Environ. Sci. Technol.* **2003**, *37* (4), 721–727.

(23) Boyanov, M. I.; O'Loughlin, E. J.; Roden, E. E.; Fein, J. B.; Kemner, K. M. Adsorption of Fe(II) and U(VI) to carboxyl-functionalized microspheres: The influence of speciation on uranyl reduction studied by titration and XAFS. *Geochim. Cosmochim. Acta* **2007**, *71* (8), 1898–1912.

(24) Wu, W. M.; Carley, J.; Fienen, M.; Mehlhorn, T.; Lowe, K.; Nyman, J.; Luo, J.; Gentile, M. E.; Rajan, R.; Wagner, D.; Hickey, R. F.; Gu, B. H.; Watson, D.; Cirpka, O. A.; Kitanidis, P. K.; Jardine, P. M.; Criddle, C. S. Pilot-scale in situ bioremediation of uranium in a highly contaminated aquifer. 1. Conditioning of a treatment zone. *Environ. Sci. Technol.* **2006**, *40* (12), 3978–3985.

(25) Brooks, S. C. *Waste Characteristics of the Former S-3 Ponds and Outline of Uranium Chemistry Relevant to NABIR Field Research Center Studies*; Report ORNL/TM-2001/27; Oak Ridge National Laboratory: Oak Ridge, TN, 2001; http://www.ornl.gov/~webworks/cppr/y2002/rpt/109994.pdf.

(26) Phillips, D. H.; Watson, D. B.; Roh, Y.; Mehlhorn, T. L.; Moon, J. W.; Jardine, P. M. Distribution of uranium contamination in weathered fractured saprolite/shale and ground water. *J. Environ. Qual.* **2006**, *35* (5), 1715–1730.

(27) Watson, D. B.; Moline, G. R.; Jardine, P. M.; Holladay, S. K.; Mehlhorn, T. L.; Gu, B.; Palumbo, A. V.; Spalding, B. P.; Brandt, C. C.; Doll, W. E. *Natural and Accelerated Bioremediation Research (NABIR) Field Research Center (FRC) Site Characterization Plan*; Report ORNL/TM-2000/269; Oak Ridge National Laboratory: Oak Ridge, TN, 2001; http://public.ornl.gov/nabirfrc/frcdoc_a.cfm.

(28) Bargar, J. R.; Reitmeyer, R.; Lenhart, J. J.; Davis, J. A. Characterization of U(VI)-carbonato ternary complexes on hematite: EXAFS and electrophoretic mobility measurements. *Geochim. Cosmochim. Acta* **2000**, *64* (16), 2737–2749.

(29) Bostick, B. C.; Fendorf, S.; Barnett, M. O.; Jardine, P. M.; Brooks, S. C. Uranyl surface complexes formed on subsurface media from DOE facilities. *Soil. Sci. Soc. Am. J.* **2002**, *66*, 99–108.

(30) Kelly, S. D.; Kemner, K. M.; Fein, J. B.; Fowle, D. A.; Boyanov, M. I.; Bunker, B. A.; Yee, N. X-ray absorption fine structure determination of pH-dependent U-bacterial cell wall interactions. *Geochim. Cosmochim. Acta* **2002**, *66* (22), 3855–3871.

(31) Merroun, M. L.; Raff, J.; Rossberg, A.; Hennig, C.; Reich, T.; Selenska-Pobell, S. Complexation of uranium by cells and S-layer sheets of Bacillus sphaericus JG-A12. *Appl. Environ. Microbiol.* **2005**, *71* (9), 5532–5543.

(32) Francis, A. J.; Gillow, J. B.; Dodge, C. J.; Harris, R.; Beveridge, T. J.; Papenguth, H. W. Uranium association with halophilic and non-halophilic bacteria and archaea. *Radiochim. Acta* **2004**, *92* (8), 481–488.

(33) Stubbs, J. E.; Elbert, D. C.; Veblen, D. R.; Zhu, C. Electron microbeam investigation of uranium-contaminated soils from Oak Ridge, TN, USA. *Environ. Sci. Technol.* **2006**, *40* (7), 2108–2113.

(34) Elzinga, E. J.; Tait, C. D.; Reeder, R. J.; Rector, K. D.; Donohoe, R. J.; Morris, D. E. Spectroscopic investigation of U(VI) sorption at the calcite-water interface. *Geochim. Cosmochim. Acta* **2004**, *68* (11), 2437–2448.

ES071764I